

Imaging organoids: a correlative light- and electron microscopy approach

Sam Willemsen

Maastricht Multimodal Imaging institute
sam.willemsen@student.maastrichtuniversity.nl

ABSTRACT

Organoids are important pharmacological and disease models. To better study organoids, existing approaches have to be adapted. Correlative microscopy approaches allow for a more holistic understanding of cellular events. While beneficial to study organoids, an effective correlative protocol for organoids has yet to be established. The current paper presents an initial correlative workflow for organoids. Two-photon light microscopy is applied to capture characteristics of organoids and co-cultured bacteria. Furthermore, 3D models and near-infrared branding are explored to guide the recovery of a region of interest for electron microscopy. Finally, different sample preparations are tested on compatibility with a correlative workflow.

Keywords

Life Sciences, Organoids, Correlative light and electron microscopy, Sample preparation, SDG 13

INTRODUCTION

Organoids are 3D structures of cells that functionally and structurally mimic a specific organ (1). They are generated from embryonic-, adult- or induced pluripotent- stem cells (1). These in vitro models are a promising alternative to animal models for pharmacology as well as for developmental and pathogenesis research (1, 2). Recently, the potential of organoids to study infection processes has been thoroughly demonstrated in both bacteria and viruses (2-4). For a comprehensive, holistic understanding of host-pathogen interactions, qualitative assessment of spatial organization by microscopy is key (5). Generally, organoids are studied through classical approaches such as immunofluorescence of sections and cell lysis followed by extraction of DNA, RNA, metabolites or proteins for use in assays (6, 7). These classical approaches yield important insights in host-pathogen interactions but are typically based on averages of bulk samples which can mask a molecular event of interest (5). Therefore, microscopy approaches provide much needed context to these classical approaches.

A promising approach for the comprehensive study of organoids is correlative light- and electron microscopy (CLEM). CLEM is an imaging approach that combines the advantages of light microscopy (LM) with the ultrastructure resolution of electron microscopy (EM). One of the advantages of CLEM, that would benefit the study of organoids, is the colocalization of a specific fluorescently tagged molecule within high resolution EM images. This enables researchers to study the biological function of a specific molecule because the higher resolution of EM can provide more detailed information on cellular- and molecular structures than possible with typical resolutions achieved with LM techniques (8). Application of CLEM to organoids infection models would also open the possibility to more effectively study

rare cellular events of host-pathogen interaction at ultrastructure resolution. Currently, rare cellular events are difficult to locate for EM applications in organoids since they are relatively large specimens. Finding the event of interest in an organoid under the high magnification of EM is like finding a needle in a haystack. However, a correlative approach that combines the fluorescent tagging of relevant molecules to locate them, followed by marking the found regions of interest (ROI) in such a way that would be visible in EM, would allow relocating these rare events in EM more efficiently. Thus, CLEM in organoids could open the way to a more detailed examination of rare events in organoid infection models by EM.

For CLEM, sample preparation should match the requirements for both LM and EM (9). Optimal existing sample preparations for fluorescent microscopy and electron microscopy for a given specimen are often not compatible. Therefore, CLEM protocols often require extensive testing of protocols for different specimens (9). To date, there has not been a detailed publication of a CLEM protocol tailored to organoids. Furthermore, for successful alignment of LM images with EM images, the orientation of the organoids in a sample should be maintained to facilitate alignment of LM and EM images. For this, a preparation method should be established that maintains organoid orientation and is compatible with LM and EM sample preparations as well. Therefore, this study aims to develop and assess a correlative workflow for organoids, focusing on different steps. Firstly, to identify an infection event through fluorescent imaging. Secondly, to mark and map the locations of infection events to relocate them for EM. Finally, to assess different sample preparation approaches on compatibility with the other steps within the overall workflow.

WORKFLOW

The workflow that was constructed for CLEM in organoids is illustrated in figure 1. Throughout this workflow, 3D models that were reconstructed from LM images were used to map ROIs and the near-infrared brandings (NIRB) that mark the ROIs in EM. The 3D models were also used to determine the relative locations of sections within the organoid, during mechanical preparation of the specimen prior to EM. Key steps in this workflow will be highlighted in the following subsections. Within these steps, the aim was to find a sample preparation compatible with both LM and EM and that maintained the orientation of the organoids. Maintaining the orientation was vital to the workflow since it was required to relocate the ROI during the mechanical preparation of the sample prior to EM. This preparation was the trimming of the sample by microtome sectioning in order to end up with specimen size and dimensions suitable for EM. The end goal of the workflow was to combine a 3D volume from LM and EM, to correlate their functional and high-resolution structural information respectively (as illustrated in the lower half of figure 1).

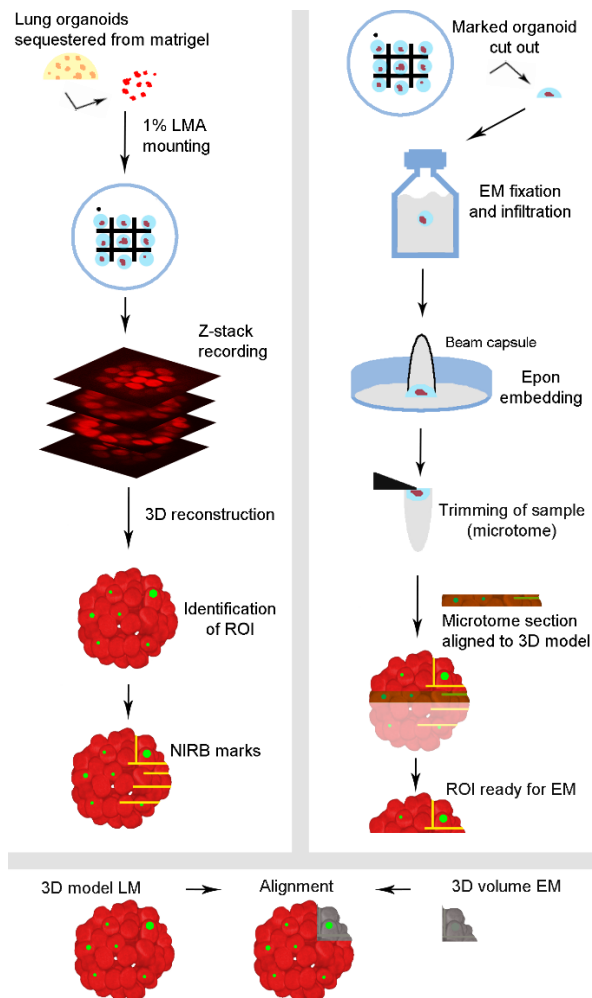


Figure 1: Visual representation of the workflow. Details presented in the text. LMA= low melting agarose, NIRB= near-infrared branding

Organoid sample preparation prior to LM

Lung organoids were kindly provided by Nino Iakobachvili from the M4i institute of Maastricht University. These organoids were established from macroscopically inconspicuous lung tissue from non-small-cell lung cancer patients. These organoids were injected with *M. marinum* expressing the mWasabi fluorophore. Interactions of these bacteria with organoid cells serve as the ROI within the workflow. Lung organoids were stained with fluorescent membrane dye ‘Concanavalin A 633’ (CF633). The differential staining was used to distinguish the bacteria from the organoid cell membranes during LM. Individual organoids were transferred to a small dish by p200 pipet, with cut off pipet tips. Three different approaches with low melting agarose (LMA) were tested in the current workflow to mount the organoids. The first approach used 1%LMA droplets while the second used 0.6%LMA droplets. The third approach used 1%LMA droplets followed by cutting out slabs of LMA containing the organoids and transferring them to glass bottles (as illustrated in figure 1).

Z-stack recording with two-photon LM

After LMA mounting, the samples were submerged in PBS and two-photon microscopy was performed on a Leica TCS SP5, equipped with a femtosecond-pulsed Ti:Sapphire laser (Chameleon, Coherent) and a 1.0 NA 20x magnification immersion objective. Z-stacks were recorded sequentially with 740nm excitation and 550-650nm emission bandwidth (for CF633) and 920nm excitation and 490-550nm emission bandwidth (for

mWasabi). Attenuation of signal in the Z-axis was corrected for by increasing PMT gain and laser strength.

Image processing and ROI identification

Z-stacks of images recorded on the two-photon system were processed in Amira 6.7. A median filter was applied to denoise the images and 3D volumes were reconstructed using the volren module. To finalize the 3D models, the bit ranges were adjusted until the 3D reconstructions were visually suitable. The 3D reconstructions were then used to identify the ROI, which were locations where signals from mWasabi and CF633 overlapped.

Marking of the ROI

An identified ROI was marked by near-infrared branding (NIRB) as described previously by Bishop et al (10). Briefly, by using high laser power at $\lambda = 800\text{nm}$ in a selected area, biological material was burned away to create small lines in the specimen. Typically, 20-40 time series were used under visual control until structural artefacts appeared. NIRB marks were confirmed by brightfield microscopy. The marks were made in the bottom of the organoids first and consecutively every $50\mu\text{m}$ higher in the Z direction. The goal was to create a recognizable pattern from the bottom of the organoid to point towards the ROI (as illustrated in figure 1). These NIRB marks were used as reference points for locating the ROIs during sample trimming.

Preparation of the organoid sample for EM

Prior to EM, the samples underwent chemical fixation and dehydration. The samples were fixated in 2.5% glutaraldehyde and 1% osmium tetroxide. Dehydration was done with a 70, 90 and 100% ethanol series. Additionally, organoids from the third LMA approach were dehydrated with propylene oxide in a glass bottle. For embedding, the samples were infiltrated overnight with an equal parts mix of epon and 100% ethanol. Subsequently, the samples were infiltrated with pure epon. Next, a thin layer of epon was left in the dish while a beam capsule filled with epon was put on top of the specimen (see figure 1). The samples were put in a stove at 60°C for 72 hours to harden the epon.

Post-embedding, the beam capsule was broken off the dish and the specimen was recovered from it. The specimens were clamped in a specimen holder and trimmed with a microtome with a glass knife (Reichert Ultracut S; Leica). Periodically, $2\mu\text{m}$ microtome sections were stained with toluidine blue and inspected under a light microscope (Labophot-2; Nikon) to assess whether the desired plane was reached and trimming should cease. This was done to find the NIRBs. Pictures of the stained sections were imaged on a Leica DM4000 B LED with a Nuance multispectral imaging system fx (CRi).

RESULTS

Mounting organoids in 1%LMA to the bottom of a dish (the first LMA approach) maintained position and orientation of the organoids during two-photon imaging. However, sectioning this sample was not possible as the sections fell apart (figure 2 A). Next, organoids were mounted in 0.6%LMA. After epon embedding, black aggregates formed in the LMA (figure 2 B). During microtome trimming, the viscosity of the black substance prevented sectioning. In the final approach, 1%LMA was used to mount the organoids to the dish. However, after two-photon imaging, slabs of LMA containing the

organoids were cut free and detached from the dish. LMA slabs were floating in fixative during embedding and could additionally be treated with propylene oxide. Using this approach, 2 to 0.1 μm thick sections were created successfully (figure 3). However, the LMA turned dark after epon embedding for some but not all samples (figure 2 C). This made organoids more difficult to locate in the epon but did not interfere with sectioning.

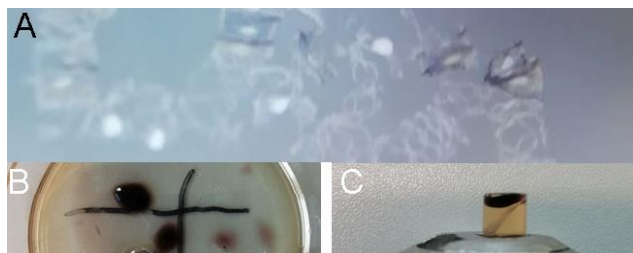


Figure 2: Complications in sample preparation during embedding for EM. (A) Thin sections of the 1%LMA sample, caught with a water bath, that fell apart and tore. (B) Black aggregates in the dish of the 0.6%LMA sample. (C) Epon block (in stub holder) containing 1%LMA slab that turned black.

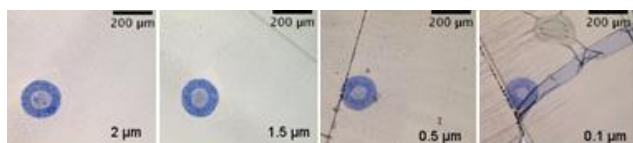


Figure 3: Microtome sections of different thickness created from the sample preparation approach of 1%LMA slabs, post epon embedding.

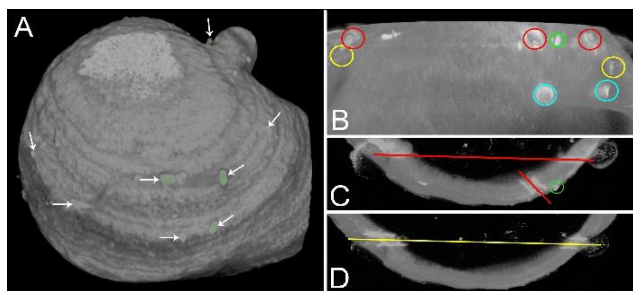


Figure 4: Localization of *m. marinum* infection event. (A) A 3D model of an organoid with a diameter of roughly 450 μm . Green fluorescence of *M. marinum* can be seen clearly at multiple locations, indicated with white arrows. The ROI is annotated in green. (B) A side view of the organoid model showing the ROI in green and the relative location of the NIRBs in red, yellow and blue. The annotated colors of the NIRBs correspond to the top-down cross-sections at different depths in the organoid, as displayed in C and D (lowest NIRBs not shown).

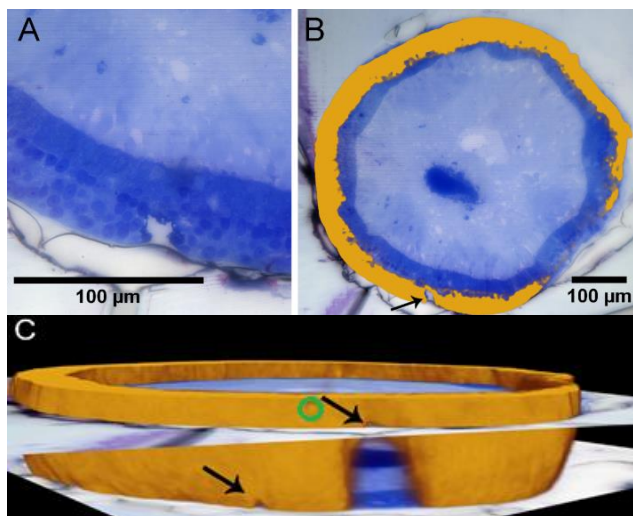


Figure 5: NIRBs found during microtome trimming and their placement in the 3D model. (A) NIRBs can be seen as holes in the tissue. Pictures are taken from 1 μm thick sections. (B) Top view of a section aligned into the organoid model (depicted in orange). (C) Side view of the organoid model with aligned NIRB sections. NIRB are indicated with arrows. ROI is indicated by a green outline.

Using two-photon microscopy images, 3D models were successfully reconstructed that showed fluorescent signal of *M. marinum*. Aggregates of this signal can be distinctly recognized in the basal side of the organoid (figure 4 A). The models showed the relative location of the fluorescent signal and thus served as a map to locate possible aggregates of *M. marinum* in the organoid in 3D. Additionally, it allowed to examine aggregates from different angles and allowed for the selection of specific sections to provide a better spatial understanding of the possible aggregates of *M. marinum*.

A NIRB pattern was created using the two-photon system to target a ROI (depicted as a green circle in figure 4 A and subfigures). After the branding was performed another z stack was recorded to create a model that includes the NIRB marks. The resulting model, as seen in figure 4 B showed the NIRBs clearly. Furthermore, the NIRBs can be clearly seen along the z-axis (figure 4 C, D). The model served as a map of the relative location of NIRBs to each other, the ROI and the rest of the organoid. It allowed for a convenient way to communicate where the NIRB marks are located within the organoids and thus guided where to look for NIRBs during trimming. Furthermore, the distance in depth between two sets of NIRB could roughly be determined by multiplying the height of the voxel with the number of slices between two points. A NIRB was targeted 320 μm deep in the organoid with an increased laser power of 50% and 60 time series but it was not recognizable in the 3D model as it did not create a distinct branding (not shown).

NIRBs were found in 1 μm sections during microtome trimming and appeared as small holes in the tissue (figure 5 A). Because organoid morphology was not symmetrical, the pictures of these sections were readily placed in the organoids 3D model. Alignment of the sections with the model revealed that the holes in the tissue aligned with the location of the NIRB (figure 5 B). Alignment of the sections revealed that there is a clear distinction between depth location, relative to other NIRBs and the ROI (figure 5 C). NIRBs were so small that they were initially overlooked during the experiment. If NIRBs were spotted during microtome sectioning they would allow for estimation of the distance to the target ROI and could thus guide the trimming of organoids.

DISCUSSION

A mounting approach was established that kept the organoids in place for two-photon microscopy, preserved organoid orientation and that was compatible with further sample preparation prior to EM. The successful mounting approach presented here consisted of attaching organoids to a dish using droplets of 1%LMA, followed by cutting out slabs of LMA containing an organoid after light microscopy. This step appeared to be necessary since 1%LMA mounted organoids that remained attached to the dish during EM embedding were not able to be sectioned during trimming, a vital step in this protocol. The advantage of the LMA slabs is most likely that the specimen is exposed to EM fixation and embedding agents from all sides, thus leading to better infiltration of the specimen. Furthermore, it could be additionally treated with propylene oxide for further dehydration because it could be transferred to a glass vial. Infiltration of a plant root sample was previously shown to be better with 0.6%LMA compared to LMA of 1% or higher (11).

However, the current study found that 0.6% LMA did not lead to a usable specimen suitable for sectioning due to the black aggregates forming in the LMA. The successful mounting approach with 1%LMA presented here showed blackening of the LMA in some cases. However, it remained possible to convincingly section these specimens up to 0.5 μm thin. The cause of the blackening of the specimens is unknown and remains a topic for further investigation.

Furthermore, 3D modeling and NIRB were used to find and subsequently map *M. marinum* infection events. While NIRBs were successfully created and later recovered during microtome sectioning, they did not lead to the recovery of the ROI in organoids. The lack of successfully trimmed lung organoid specimens was partly due to difficulty in recognizing NIRB during microtome sectioning because of their small size. The NIRBs were so small that they were overlooked during the microtome trimming. NIRBs need to be recognized during sectioning to assess at how much of the organoid has been trimmed away and to approximate how near the ROI is. However, placement of a 2 μm slice in the 3D model, after the specimen was used up, indicated how deep in the organoid the section was trimmed. Therefore, this placement (as illustrated in figure 5 C) would allow the researcher to judge if the distance to the next NIRB or the ROI is close or far, thus guiding the trimming process. Instrumental in this is the convenience of 3D models of the organoid, as these maps provide an accessible way to interpret and communicate the relative locations of the NIRBs in an organoid. Finally, NIRBs of a larger depth and size would make it more likely that NIRB marks are encountered during sectioning and not missed because of loss of a section during handling or due to being overlooked by the researcher.

CONCLUSION

The current study presents an initial correlative approach to organoid imaging. A successful sample preparation was found that supports two-photon imaging, epon embedding, microtome sectioning, and EM while maintaining the organoids orientation. Furthermore, NIRBs were created in organoids to mark an ROI and were successfully mapped into 3D models that provided an accessible way to interpret and communicate the relative locations of NIRBs and the ROI in an organoid. The NIRBs can guide microtome trimming to create suitably prepared specimens prior to EM if they are recovered during the sample trimming. The workflow presented here has the potential to lead to a more effective study of infection events and other rare cellular events in organoids at high resolutions of EM. It puts forward a solution to the ‘needle in the haystack’ problem by utilizing the functional information gained by LM to guide relocation of a ROI in EM. However, further experiments and optimization are required to overcome the current limitations of the workflow.

ROLE OF THE STUDENT

Sam Willemsen was an undergraduate student working under the supervision of Kèvin Knoops when the research in this report was performed. The topic was proposed by the supervisor. The testing and execution of the workflow, processing of images and results as well as formulation of the conclusions and the writing were done by the student.

ACKNOWLEDGMENTS

I would like to thank Nino Iakobachvili (M4i) for culturing the lung organoids. Furthermore, I thank Willine van de Wetering (M4i) and Hans Duimel (M4i) for assisting with sample preparation steps for EM as well as for sharing some of their expertise during the construction of the workflow. I want to thank Helma Kuijpers (M4i) for familiarizing me with the laboratory and microscopes. Finally, I want to thank Kèvin Knoops (M4i) for supervising this project.

REFERENCES

1. Clevers H. Modeling Development and Disease with Organoids. *Cell*. 2016;165(7):1586-97.
2. Sachs N, Papaspyropoulos A, Zomer-van Ommen DD, et al. Long-term expanding human airway organoids for disease modeling. *EMBO J*. 2019;38(4).
3. Fonseca KL, Rodrigues PNS, Olsson IAS, et al. Experimental study of tuberculosis: From animal models to complex cell systems and organoids. *PLoS Pathog*. 2017;13(8):e1006421.
4. Mills M, Estes MK. Physiologically relevant human tissue models for infectious diseases. *Drug Discov Today*. 2016;21(9):1540-52.
5. Laketa V. Microscopy in Infectious Disease Research-Imaging Across Scales. *J Mol Biol*. 2018;430(17):2612-25.
6. O'Donnell N, Dmitriev RI. Three-Dimensional Tissue Models and Available Probes for Multi-Parametric Live Cell Microscopy: A Brief Overview. *Adv Exp Med Biol*. 2017;1035:49-67.
7. Zhang YG, Wu S, Xia Y, et al. Salmonella-infected crypt-derived intestinal organoid culture system for host-bacterial interactions. *Physiol Rep*. 2014;2(9).
8. de Boer P, Hoogenboom JP, Giepmans BN. Correlated light and electron microscopy: ultrastructure lights up! *Nat Methods*. 2015;12(6):503-13.
9. Ando T, Bhamidimarri SP, Breeding N, et al. The 2018 correlative microscopy techniques roadmap. *J Phys D Appl Phys*. 2018;51(44):443001.
10. Bishop D, Nikic I, Brinkoetter M, et al. Near-infrared branding efficiently correlates light and electron microscopy. *Nat Methods*. 2011;8(7):568-70.
11. Wu S, Baskin TI, Gallagher KL. Mechanical fixation techniques for processing and orienting delicate samples, such as the root of *Arabidopsis thaliana*, for light or electron microscopy. *Nat Protoc*. 2012;7(6):1113-24.
12. Maco B, Holtmaat A, Cantoni M, et al. Correlative in vivo 2 photon and focused ion beam scanning electron microscopy of cortical neurons. *PLoS One*. 2013;8(2):e57405.
13. Blazquez-Llorca L, Hummel E, Zimmerman H, et al. Correlation of two-photon in vivo imaging and FIB/SEM microscopy. *J Microsc*. 2015;259(2):129-36.

“Permission to make digital or hard copies of all or part of this work for personal or classroom use is granted under the conditions of the Creative Commons Attribution-Share Alike (CC BY-SA) license and that copies bear this notice and the full citation on the first page”

SRC 2019, December 5, 2019, The Netherlands.